to the trans diradial Cl(1)-Ta(1)-C(1) angle of 129.5 (3)°.

The distribution of observable ligands about the two tantalum atoms is clearly shown in Figure 2; the μ-hydride ligand bridges an axial site on Ta(2) and a radial site on Ta(1). The Ta(μ-H)(μ-CHO)Ta core may be drawn as in **8**.

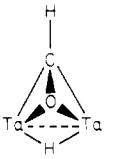

8

We now come to a consideration of the bridging formyl ligand. As shown in Figure 3, this ligand (although not occupying equivalent sites on the two tantalum atoms; vide supra) appears to bonded to the two tantalum atoms with essentially equivalent metal-ligand distances (Å): Ta(1)-C(1) = 2.085 (12) and Ta(2)-C(1) = 2.119 (11); Ta(1)-O = 2.094 (8) and Ta(2)-O = 2.089 (9). The Ta(1)-C(1)-Ta(2) and Ta(1)-O-Ta(2) angles are (respectively) 98.6 (5) and 99.2 (4)°; the Ta(1)-[C(1)-O]-Ta(2) system has a "butterfly" geometry in which the Ta(1)-C(1)-O plane is displaced by 71.15° from coplanarity with the Ta(2)-C(1)-O system.

The C(1)-O distance of 1.496 (14) Å is unusually long for a carbon-oxygen single bond. (The average C-O bond length in alcohols, ethers, or epoxides is 1.43 Å;[18] Pauling[19] suggests r(C) = 0.772 Å and r(O) = 0.66 Å, also predicting d(C-O) = 1.43 Å.) This activation of the C(1)-O bond is consistent with the observation that it is cleaved by attack of PMe_3 on C(1) [see last step of Scheme I].

All other distances and angles in the molecule are normal.

Acknowledgment. This work has been supported by the National Science Foundation (Grant CHE80-23448, to M.R.C.). We are most grateful to Patricia Belmonte for her persistent efforts in obtaining crystals of this complex and to Professor R. R. Schrock for his continuing interest in these studies.

Registry No. 4, 74167-06-9.

Supplementary Material Available: A listing of observed and calculated structure factor amplitudes (21 pages). Ordering information is given on any current masthead page.

(18) "Interatomic Distances", *Spec. Publ.-Chem. Soc.* **1965**, *No. 18*, S20s.
(19) Pauling, L. "The Nature of the Chemical Bond", 3rd ed.; Cornell University Press: Ithaca, NY, 1960; Table 7-2, p 224.

Contribution from the Department of Chemistry, University of Arizona, Tucson, Arizona 85721, and Laboratoire de Chimie de Coordination du CNRS, Associé à l'Université Paul Sabatier, 31400 Toulouse, France

Oxygen Atom Transfer Reactions. 2. Reaction of Carbon Monoxide with $Ni(NO_2)_2(PMe_3)_2$: Structure of Nitronitrosylbis(trimethylphosphine)nickel, $Ni(NO_2)(NO)(PMe_3)_2$

J. KRIEGE-SIMONDSEN,[1a] G. ELBAZE,[1b] M. DARTIGUENAVE,[1b] R. D. FELTHAM,*[1a] and Y. DARTIGUENAVE[1b]

Received May 19, 1981

The reaction between CO and $Ni(NO_2)_2(PMe_3)_2$, which forms CO_2 and $Ni(NO_2)(NO)(PMe_3)_2$ as final products, is associative and indicates the presence of $Ni(NO_2)_2(CO)(PMe_3)_2$ as an intermediate or transition state. The crystal and molecular structure of $Ni(NO_2)(NO)(PMe_3)_2$ has been determined by single-crystal X-ray diffraction at 293 and 135 K. This compound crystallizes in the monoclinic space group C_{2h}^5 - $P2_1/c$ with four molecules in a unit cell of dimensions a = 7.751 (2) Å, b = 12.611 (3) Å, c = 14.328 (4) Å, and β = 96.93 (3)° at 293 K and a = 7.648 (5) Å, b = 12.468 (11) Å, c = 13.956 (11) Å, and β = 95.88 (6)° at 135 K. Full-matrix least-squares refinement of the 293 K data set based on 1811 unique reflections having $F_o^2 > 3\sigma(F_o^2)$ converged with R_1 = 0.0456 and R_2 = 0.0713. The room-temperature structure consists of discrete $Ni(NO_2)(NO)(PMe_3)_2$ molecules with distorted tetrahedral geometry about the nickel atom. The P-Ni-P angle is 106.06 (7)°, and the N-Ni-N angle is 126.2 (3)°. Important interatomic distances are Ni-P(1) = 2.243 (2), Ni-P(2) = 2.243 (2), Ni-N(O_2) = 1.997 (6), and Ni-N(O) = 1.652 (7) Å. Except for the significantly shortened distance of 2.228 (3) Å found for Ni-P(1), the bond distances at 135 K do not differ from those at 293 K. Only minor differences in the bond angles were noted. The thermal parameters of the nitrosyl oxygen atom, O(3), are decreased significantly, with no indication of disorder of the nitrosyl ligand. The nonequivalent Ni-P distances observed at 135 K may be evidence of vibronic coupling with low-lying excited states of the complex.

Introduction

The recent isolation of pentacoordinate monocarbonyl complexes of divalent nickel, $NiX_2(CO)(PR_3)_2$ (X = halide; PR_3 = PMe_3, PMe_2Ph, $PMePh_2$, PPh_3), and the structural characterization of one of them,[2a] $Ni(CO)I_2(PMe_3)_2$, have prompted us to examine the reaction of $Ni(NO_2)_2(PMe_3)_2$ with CO.

The reaction of CO with the closely related complexes $Ni(NO_2)_2(PEt_3)_2$[2b,3] and $Ni(NO_2)_2(DPPE)$[4] (DPPE = $Ph_2PCH_2CH_2PPh_2$) has been studied in some detail and has been shown to proceed via reaction 1. Kinetic evidence

$$Ni(NO_2)_2L_2 + CO \rightarrow Ni(NO_2)(NO)L_2 + CO_2 \quad (1)$$

(1) (a) University of Arizona. (b) l'Université Paul Sabatier.
(2) (a) Saint-Joly, C.; Mari, A.; Gleizes, A.; Dartiguenave, M.; Dartiguenave, Y.; Galy, J. *Inorg. Chem.* **1980**, *19*, 2403. Saint-Joly, C.; Dartiguenave, M.; Dartiguenave, Y. *Adv. Chem. Ser.* **1979**, *No. 173*, 152. (b) Booth, G.; Chatt, J. *J. Chem. Soc.* **1962**, 2099.
(3) Doughty, D. T.; Gordon, G.; Stewart, R. P. *J. Am. Chem. Soc.* **1979**, *101*, 2645.
(4) Feltham, R. D.; Kriege, J. *J. Am. Chem. Soc.* **1979**, *101*, 5064.

0020-1669/82/1321-0230$01.25/0

Table I. Rate of Reaction of $Ni(NO_2)_2(PMe_3)_2$ with Carbon Monoxide in Benzene at 22 °C Shown as $-\ln (A_\infty - A_t)$

time, min	P_{CO}, atm				
	0.130	0.340	0.429	0.623	0.89
2			0.243	0.365	
3			0.393	0.540	0.782
4		0.340	0.519	0.696	1.02
5		0.449	0.630	0.874	1.30
6		0.536	0.790	1.07	1.66
7		0.675	0.930	1.26	1.86
8	0.260	0.764	1.05	1.46	2.16
9	0.360	0.904	1.23	1.68	2.47
10	0.441	1.052	1.35	1.86	2.82
11	0.475	1.085	1.49	1.96	3.00
12	0.527	1.150	1.60	2.11	3.29
13	0.575	1.25	1.73		
14	0.623	1.31			
15	0.707	1.42			
16	0.760	1.52			
17	0.838	1.73			
18	0.850	1.79			

strongly indicated the formation of the pentacoordinate intermediate[4] $Ni(CO)(NO_2)_2L_2$ during reaction 1,[4] and ^{18}O labeling[3] of $Ni(NO_2)_2(PEt_3)_2$ proved that the NO_2 ligand is the source of oxygen in the oxidation of CO to CO_2. However, the proposed pentacoordinate intermediate was not experimentally observed in these prior studies. Our previous experience with the fixation of CO by $NiX_2(PR_3)_2$ indicated that the pentacoordinate monocarbonyl complexes with trimethylphosphine were the most stable and therefore offered the best opportunity to observe directly the pentacoordinate intermediate proposed for reaction 1. Thus, the present study of the reaction of CO with *trans*-$Ni(NO_2)_2(PMe_3)_2$, including rate studies and structural characterization of the products reported below, was initiated.

Experimental Section

Materials. $Ni(NO_2)(NO)(PMe_3)_2$ (**1**) was prepared from the reaction of 0.7 g (2.5 mmol) of $Ni(NO_2)_2(PMe_3)_2$ (**2**)[5] with CO in 20 mL of carefully degassed acetone. After CO was bubbled through the acetone solution of **2** for 2 h (20 °C; 1 atm), a dark purple solution was obtained. After evaporation of the solvent under vacuum, the dark residue was dissolved in diethyl ether (30 mL), filtered, and cooled to −30 °C under an atmosphere of CO. After 3 h, the well-formed crystals were collected by filtration and dried in a stream of CO. Several crystals of suitable size were coated with stopcock grease, and mounted in capillaries, and sealed under nitrogen.

IR: ν_{NO} = 1718 cm^{-1}. ^{31}P NMR: −0.05 ppm (relative to 62.5% H_3PO_4). Visible absorption bands: 2.80, 2.25, and 1.75 μm^{-1}. Anal. Calcd for $C_6H_{18}N_2NiO_3P_2$: C, 25.1; H, 6.32; N, 9.76. Found: C, 25.1; H, 6.32; N, 9.48.

Rate Measurement. The rate of the reaction of CO with **2** (Table I) was monitored by measuring the increase in peak intensity of ν_{NO} of **1** vs. time. A calibration curve for ν_{NO} vs. C (mmol L^{-1}) was prepared for various concentrations of **1** in benzene. Carbon monoxide at 22 °C and 1 atm was mixed rapidly with a solution of **2** in benzene (7.01 mmol L^{-1}; 22 °C). Lower partial pressures of CO were obtained by dilution with N_2. The CO content of these mixtures was determined by gas chromatography. The solubility of carbon monoxide at 22 °C determined experimentally (β = 120 atm L mol^{-1}) is in substantial agreement with the value reported by Linke (β = 134 atm L mol^{-1}).[6]

Collection and Reduction of X-ray Intensity Data. A crystal of **1** was mounted on a Syntex $P2_1$ autodiffractometer equipped with a scintillation counter, a graphite monochromator, and a Syntex LT1 low-temperature device. The longest dimension of the crystal (b axis) was approximately parallel to the ϕ axis. Automatic centering, indexing, and least-squares routines were carried out to yield the cell dimensions that are listed in Table II together with other crystallographic data.[7] Intensity data were collected at room temperature under the conditions listed in this table. The data were reduced to F_o^2 and $\sigma(F_o^2)$ by published procedures. Lorentz polarization factors were calculated on the assumption of 50% mosaicity and and 50% perfection of the monochromator crystal. During the data collection, all three standards showed a 5% or less decline in intensity. Because of these small intensity changes and the equidimensional shape of the crystal, corrections for decomposition and absorption were not significant.

Solution and Refinement of the Structure. Neutral-atom scattering factors for the nonhydrogen atoms and corrections for the anomalous dispersion made for the nickel and phosphorus atoms were taken from the tabulations of Cromer and Waber.[8] The hydrogen atom scattering factors were taken from the calculations of Stewart, Davidson, and Simpson.[9] The structures were refined by full-matrix least-squares techniques minimizing the function[9] $\sum w(|F_o| - |F_c|)^2$ where $w = 4F_o/[\sigma^2(F_o^2) + (pF_o^2)^2]$. "$P$", the factor to prevent overweighting strong reflections, was set equal to 0.03. The discrepancy indices, R_1 and R_2, are defined in the usual way.

The room-temperature structure was solved by the heavy-atom method in which the position of the nickel atom was readily determined from a three-dimensional Patterson map. The remaining nonhydrogen atoms were located by successive refinements and difference electron density maps. Refinement of this structure with anisotropic thermal parameters for all atoms converged with R_1 = 0.0608 and R_2 = 0.0952. At this point, the positions of six hydrogen atoms labeled (1) in Table V were located from a series of difference electron density maps. The remaining 12 hydrogen atoms were placed at geometrically idealized positions (C–H = 0.95 Å). All hydrogen atoms were assigned an isotropic temperature factor, B = 5.0 $Å^2$, and were held fixed in subsequent refinements. Final refinements of this model using the 1811 independent reflections (Tables III and IV) (Table IV is supplementary material) with $F_o^2 \geq 3\sigma(F_o^2)$ and $2\theta \leq 50°$ converged with R_1 = 0.0456 and R_2 = 0.0713. All parameter shifts during the final cycle of refinement were less than 0.05σ. The "goodness of fit", defined by $[\sum w(|F_o| - |F_c|)^2/(n-m)]^{1/2}$ where n is the number of reflections used in the refinement and m is the number of refined parameters, was 2.917. The overdetermination ratio (n/m) was 14.3. The largest peak in the final electron density map was 0.497 e $Å^{-3}$. The temperature factors for the O atom of the nitrosyl group were large, suggestive of possible disorder common in nonlinear metal nitrosyl complexes.[10] Consequently, intensity data were collected from the same crystal at 135 K, with the conditions listed in Table II. Lower supplied power and faster scanning speed resulted in slightly fewer data being observed at 135 K than at 293 K. The low-temperature structure was solved by using the coordinates of the nonhydrogen atoms from the room-temperature model followed by least-squares refinements and difference electron density maps which revealed the positions of all 18 hydrogen atoms. All atoms were then refined to isotropic convergence. The positions of the hydrogen atoms were then held fixed while the remaining atoms were refined to anisotropic convergence. The final cycle of refinement,[11] based on the 1512 unique reflections having $F_o^2 \leq 3\sigma(F_o^2)$, converged with R_1 = 0.0526 and R_2 = 0.0544. All parameter shifts during the final cycle of refinement were less than 0.04σ. The "goodness of fit" was 1.808, and the largest peak in the final electron density map (1.55 e $Å^{-3}$) was 1.07 Å from

(5) Merle, A.; Dartiguenave, M.; Dartiguenave, Y. *Bull. Soc. Chim. Fr.* **1972**, 87.
(6) Linke, W. F. "Solubilities of Inorganic and Metal-Organic Compounds", 4th ed.; American Chemical Society: Washington, D. C., 1958; vol. 1, p 456.
(7) Programs used for centering of reflections, autoindexing, least-squares refinement of cell parameters, and data collection are in: "Syntex $P2_1$ Fortran Operation Manual"; Syntex Analytical Instruments: Cupertino, CA, 1975.
(8) Cromer, D. T.; Waber, J. T. "International Tables for X-Ray Crystallography"; Ibers, J. A., Hamilton, W. C., Eds.; Kynoch Press: Birmingham, England, 1974; vol. IV, Table 2.2A, p 149. Cromer, D. T. *Ibid.*, Table 231 p 149.
(9) Davidson, E. R.; Simpson, W. L. *J. Chem. Phys.* **1965**, *42*, 3175.
(10) Johnson, P. L.; Enemark, J. H.; Feltham, R. D.; Swedo, K. B. *Inorg. Chem.* **1976**, *15*, 2989.
(11) All computations were carried out on the CDC CY-175 computer at the University of Arizona Computer Center. The major programs used for the structure determination were FORDAP (Fourier summation program by A. Zalkin), Ibers' NUCLS (Structure factor calculations and full-matrix least-squares refinement, a modification of ORFLS by W. R. Busing, K. O. Martin, and H. A. Levy), ORFFE (locally modified calculation of distances, angles, and least-squares planes with standard deviations by W. R. Busing, K. O. Martin, and H. A. Levy) and ORTEP (thermal ellipsoid drawing program by C. K. Johnson).

Table II. Crystallographic Data

	293 K[a]	135 K[a]
molecular formula	$[Ni(NO_2)(NO)(P(CH_3)_3)_2]$	$[Ni(NO_2)(NO)(P(CH_3)_3)_2]$
mol wt	283.36	283.36
cryst shape	cubic	cubic
cryst dimens, mm^3	$0.35 \times 0.38 \times 0.47$	
cryst system	monoclinic	monoclinic
cell dimens[b]		
a, Å	7.751 (2)	7.648 (5)
b, Å	12.611 (3)	12.468 (11)
c, Å	14.328 (4)	13.956 (11)
β, deg	96.93 (3)	95.88 (6)
V, $Å^3$	1390.3 (6)	1324 (2)
Z	4	4
d_{obsd},[c] $g\ cm^{-3}$	1.33 (3)	
d_{calcd}, $g\ cm^{-3}$	1.37	1.30
radiation, Å	(Mo Kα) 0.7103	(Mo Kα) 0.7103
monochromator	graphite crystal	graphite crystal
supplied power	50 kV, 30 mA	50 kV, 25 mA
data collection method	θ-2θ scan	θ-2θ scan
scan speed, deg min^{-1}	variable, 2.00–29.30, determined as a function of peak intensity	variable, 3.00–29.30, determined as a function of peak intensity
ratio of total bkgd time to peak scan time	0.5	0.5
scan range (2θ), deg	Mo K_1 −0.8 to Mo K_2 +0.8	Mo K_1 −0.8 to Mo K_2 +0.8
std reflctns	(200), (020), (004) after every 97 readings	(200), (020), (004) after every 97 readings
decompn of standards	5%	3%
2θ limit, deg	0.0–50.0	0.0–50.0
no. of unique data	2584	2481
no. of data used in the calcn	1811	1515, $I > 3\sigma(I)$
abs coeff (μ), cm^{-1}	15.79 (Mo Kα)	15.79 (Mo Kα)

[a] The standard deviation of the least significant figure is given in parentheses in this and the following tables. [b] Cell dimensions were obtained from a least-squares refinement of setting angles of 25 reflections in the 2θ range 5–25°. [c] Density was determined by flotation using a solution of diethyl ether and carbon tetrachloride.

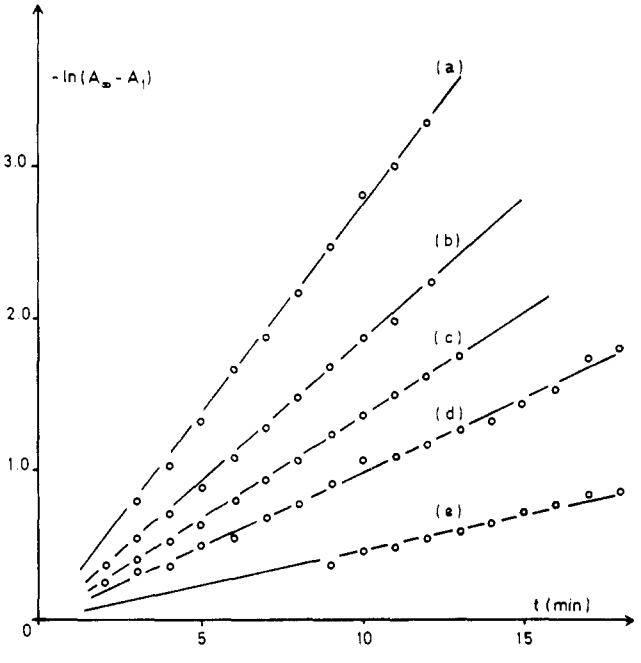

Figure 1. Plots of $-\ln(A_\infty - A_t)$ vs. *t* (22 °C, 1 atm, benzene solvent) for the reaction of CO with $Ni(NO_2)_2(PMe_3)_2$ at P_{CO} = 0.89 (a), 0.623 (b), 0.429 (c), 0.340 (d), and 0.130 (e) atm.

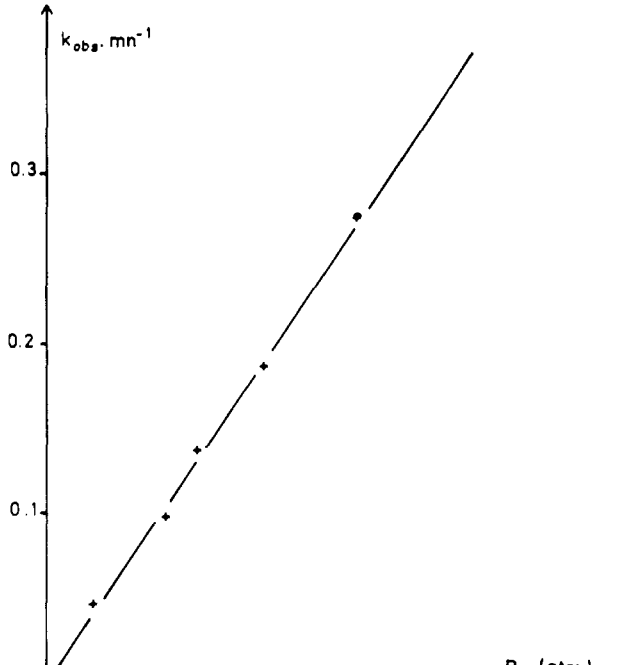

Figure 2. Dependence of k_{obsd} on P_{CO} (22 °C, benzene) for the reaction of CO with $Ni(NO_2)_2(PMe_3)_2$.

Ni. The overdetermination ratio was 11.9.

Results

Synthesis and Reaction with Carbon Monoxide. The reaction of **2** with carbon monoxide in dry, oxygen-free benzene rapidly produced a deep purple solution, from which the dark purple crystalline complex $Ni(NO_2)(NO)(PMe_3)_2$ was isolated in nearly quantitative yield. The compound was characterized by elemental analysis, by infrared, UV–visible, and $^{31}P\{^1H\}$ NMR spectroscopy, and by the single-crystal X-ray structure determination.

Spectroscopic investigation of the solution during the reaction indicated the presence of only two nickel species: $Ni(NO_2)_2(PMe_3)_2$ and $Ni(NO_2)(NO)(PMe_3)_2$. The stoichiometry of this reaction also corresponds to reaction 1. The rate of this reaction in benzene was measured at 22 °C by following the appearance of the NO stretching frequency of the $\{NiNO\}^{10}$ product at 1718 cm^{-1}. The reaction rate has been determined at several CO pressures (Figure 1 and Table I). The reaction is first order in $Ni(NO_2)_2(PMe_3)_2$ at constant

Table III. Atomic Positional Parameters for the Nonhydrogen Atoms of $Ni(NO_2)(NO)(P(CH_3)_3)_2$

atom	x		y		z	
	293 K	135 K	293 K	135 K	293 K	135 K
Ni	0.2329 (1)	0.2394 (1)	0.15156 (6)	0.14685 (7)	0.18590 (5)	0.1834 (6)
P(1)	0.3052 (2)	0.3073 (2)	0.1491 (1)	0.1461 (1)	0.3422 (1)	0.3425 (1)
P(2)	−0.0535 (2)	−0.0497 (2)	0.1842 (1)	0.1821 (1)	0.1623 (1)	0.1618 (1)
N(1)	0.3131 (8)	0.3172 (7)	0.2983 (5)	0.2958 (5)	0.1613 (4)	0.1582 (4)
N(2)	0.2875 (9)	0.2960 (8)	0.0422 (5)	0.0352 (5)	0.1332 (4)	0.1313 (4)
O(1)	0.2197 (8)	0.2207 (6)	0.3785 (4)	0.3763 (4)	0.1640 (4)	0.1628 (4)
O(2)	0.4576 (7)	0.4677 (6)	0.3099 (5)	0.3103 (4)	0.1350 (5)	0.1329 (4)
O(3)	0.2977 (14)	0.3129 (10)	−0.0436 (6)	−0.0534 (5)	0.1055 (7)	0.1047 (5)
C(1)	0.1739 (11)	0.1719 (10)	0.0638 (7)	0.0606 (6)	0.4066 (5)	0.4099 (5)
C(2)	0.2977 (11)	0.2959 (10)	0.2758 (5)	0.2761 (6)	0.3986 (5)	0.3987 (5)
C(3)	0.5214 (10)	0.5279 (9)	0.1048 (7)	0.1026 (6)	0.3815 (6)	0.3851 (6)
C(4)	−0.1363 (9)	−0.1329 (9)	0.2733 (7)	0.2719 (7)	0.2463 (5)	0.2484 (5)
C(5)	−0.1290 (9)	−0.1236 (9)	0.2437 (6)	0.2442 (6)	0.0502 (5)	0.0482 (5)
C(6)	−0.1908 (12)	−0.1935 (10)	0.0700 (7)	0.0667 (6)	0.1639 (7)	0.1632 (6)

[a] x, y, and z are in fractional monoclinic coordinates.

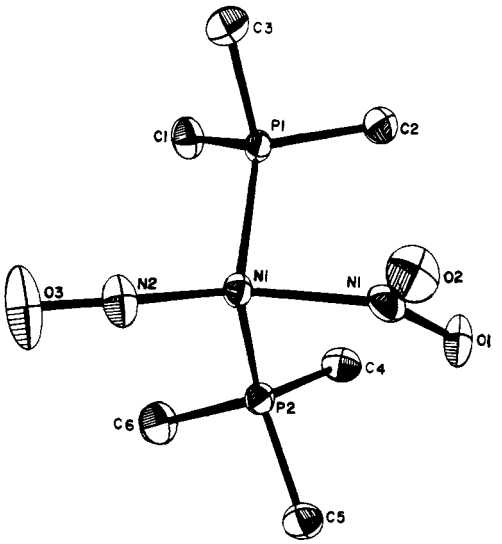

Figure 3. ORTEP drawing of $Ni(NO_2)(NO)(PMe_3)_2$ at 135 K.

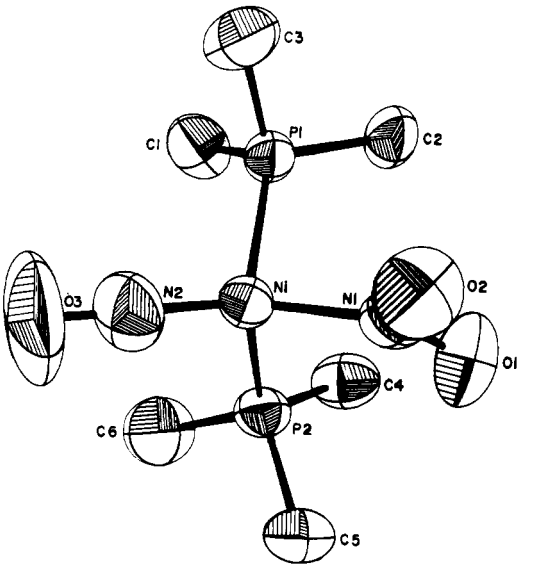

Figure 4. ORTEP drawing of $Ni(NO_2)(NO)(PMe_3)_2$ at 293 K.

CO pressure since $\log [1/(1 + x)]$ vs. time is linear. The CO concentration was varied over a limited range, and a plot of K_{obsd} vs. P_{CO} is linear (Figure 2). Thus the rate law $-d[Ni(NO_2)_2(PMe_3)_2]/dt = k[Ni(NO_2)(NO)(PMe_3)_2][CO]$ is applicable and gives a value of $k_2 = 6.0 \times 10^{-1}$ L mol^{-1} s^{-1} at 22 °C.

Description of the Structure. The interatomic distances and angles found for the nonhydrogen atoms of **1** at both 293 and 135 K are set out in Table VI. A perspective view and the numbering scheme for the molecules at 135 and 293 K are shown in Figures 3 and 4. The root-mean-square amplitudes of vibration for the nonhydrogen atoms are listed in Table VII (supplementary material) while the thermal and positional parameters for the hydrogen atoms are found in Table V.

At both temperatures, the crystal structure of **1** consists of discrete $Ni(NO_2)(NO)(PMe_3)_2$ molecules with the closest intermolecular contacts of 2.761 and 2.437 Å found between O(1) and 1H(1). The crystal packing of these molecules at 135 and 293 is shown in Figure 5. At 135 K, the nonbonded intramolecular distances are of the order of van der Waals distances, and all hydrogen–hydrogen contacts are 2.378 Å or greater. No evidence was found for interaction between the oxygen atoms of adjacent molecules with nickel atoms of adjoining molecules.

Room-Temperature Form. The coordination geometry about the nickel atom is significantly distorted from tetrahedral. Although the P(1)–Ni–P(2) angle of 106.06 (7)° is only slightly smaller than that of a regular tetrahedron, the N-(1)–Ni–N(2) angle of 126.2 (3)° is considerably greater. The dihedral angle of 90.4° between the P–Ni–P and N–Ni–N planes differs only slightly from the idealized angle of 90° for the regular tetrahedron. The two Ni–P bond lengths are the same (2.243 (2) Å). The Ni–N(O) bond length of 1.652 (7) Å is among the shortest M–N(O) bond lengths that have been

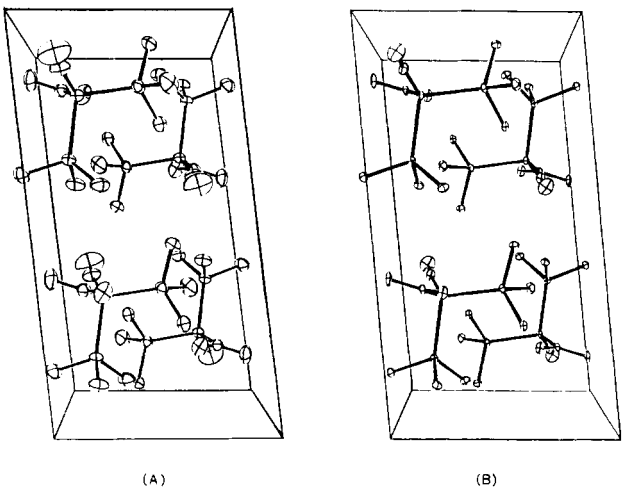

Figure 5. Packing diagram for $Ni(NO_2)(NO)(PMe_3)_2$ at 293 K (a) and 135 K (b).

Table V. Thermal and Positional Parameters for the Hydrogen Atoms of $Ni(NO_2)(NO)(P(CH_3)_3)_2$[a]

	x		y		z		B, Å²	
atom	293 K	135 K	293 K	135 K	293 K	135 K	293 K	135 K
1H(1)	0.2322	0.2120	0.0586	0.0835	0.4804	0.4916	5.00	6.58
1H(2)	0.1632	0.1945	−0.0068	0.0080	0.3812	0.3872	5.00	1.59
1H(3)	0.0560	0.0626	0.0908	0.0711	0.4065	0.3805	5.00	2.10
2H(1)	0.3331	0.3200	0.2777	0.2776	0.4511	0.4643	5.00	2.15
2H(2)	0.1789	0.1711	0.2988	0.3055	0.3942	0.3800	5.00	4.53
2H(3)	0.3618	0.3895	0.3257	0.3174	0.3671	0.3605	5.00	2.92
3H(1)	0.6096	0.6138	0.1365	0.1551	0.3496	0.3638	5.00	3.32
3H(2)	0.5320	0.5344	0.0298	0.0460	0.3739	0.3703	5.00	2.84
3H(3)	0.5523	0.5341	0.1209	0.1110	0.4472	0.4561	5.00	0.67
4H(1)	−0.2394	−0.2354	0.2748	0.2851	0.2287	0.2303	5.00	0.13
4H(2)	−0.0877	−0.0699	0.3451	0.3323	0.2400	0.2500	5.00	1.70
4H(3)	−0.1077	−0.1119	0.2518	0.2395	0.3084	0.3223	5.00	2.31
5H(1)	−0.2457	−0.2315	0.2486	0.2529	0.0541	0.0526	5.00	7.42
5H(2)	−0.1057	−0.0976	0.2032	0.2044	0.0014	−0.0136	5.00	1.75
5H(3)	−0.0847	−0.0593	0.3141	0.2942	0.0484	0.0405	5.00	2.62
6H(1)	−0.2675	−0.3229	0.0818	0.0985	0.1616	0.1431	5.00	5.98
6H(2)	−0.1585	−0.1858	0.0291	0.0369	0.2210	0.2301	5.00	2.03
6H(3)	−0.1739	−0.1854	0.0229	0.0190	0.1121	0.1099	5.00	4.16

[a] In the case of the structure determination at 25 °C, all hydrogen atoms labeled with a "(1)" were located on a difference electron density map while those labeled with a "(2)" or a "(3)" were placed at geometrically idealized positions. All of these hydrogen atoms were assigned an isotropic temperature factor, $B = 5.00$ Å². All hydrogen parameters were held fixed during refinement in the case of structure determination at 25 °C. For the structure determination at −138 °C, all hydrogen atoms were located on a series of difference electron density maps. Parameters for these hydrogen atoms were allowed to vary while the structure was refined to isotropic convergence. Parameters were then held fixed while the structure was converged with anisotropic thermal parameters on all nonhydrogen atoms.

Table VI. Interatomic Distances and Angles[a]

Distances

atoms	293 K	135 K	atoms	293 K	135 K
Ni-P(1)	2.243 (2)	2.228 (3)	P(1)-C(1)	1.808 (7)	1.814 (7)
Ni-P(2)	2.243 (2)	2.244 (2)	P(1)-C(2)	1.795 (7)	1.807 (7)
Ni-N(1)	1.997 (6)	1.992 (6)	P(1)-C(3)	1.791 (8)	1.813 (7)
Ni-N(2)	1.652 (7)	1.648 (6)	P(2)-C(4)	1.820 (8)	1.810 (8)
N(1)-O(1)	1.247 (7)	1.252 (7)	P(2)-C(5)	1.805 (7)	1.803 (7)
N(1)-O(2)	1.233 (7)	1.251 (7)	P(2)-C(6)	1.792 (8)	1.812 (7)
N(2)-O(3)	1.158 (8)	1.177 (7)			

Angles

atoms	293 K	135 K	atoms	293 K	135 K
N(1)-Ni-N(2)	126.2 (3)	127.8 (3)	C(1)-P(1)-C(2)	104.4 (4)	104.2 (3)
N(1)-Ni-P(1)	98.3 (1)	97.8 (2)	C(1)-P(1)-C(3)	102.6 (4)	102.5 (4)
N(1)-Ni-P(2)	97.3 (2)	95.8 (2)	C(1)-P(1)-Ni	115.4 (2)	115.6 (3)
N(2)-Ni-P(1)	113.4 (2)	113.0 (2)	C(2)-P(1)-C(3)	102.5 (5)	102.1 (3)
N(2)-Ni-P(2)	112.8 (2)	114.0 (2)	C(2)-P(1)-Ni	114.8 (2)	114.3 (2)
P(1)-Ni-P(2)	106.06 (7)	105.1 (1)	C(3)-P(1)-Ni	115.5 (3)	116.2 (3)
O(1)-N(1)-O(2)	117.7 (6)	117.6 (6)	C(4)-P(2)-C(5)	103.2 (3)	102.8 (3)
Ni-N(1)-O(1)	123.5 (5)	123.4 (4)	C(4)-P(2)-C(6)	103.3 (4)	103.2 (4)
Ni-N(1)-O(2)	118.5 (5)	119.0 (5)	C(4)-P(2)-Ni	115.8 (2)	116.1 (2)
Ni-N(2)-O(3)	165.5 (8)	166.9 (6)	C(5)-P(2)-C(6)	102.5 (4)	102.4 (4)
			C(5)-P(2)-Ni	114.8 (2)	114.7 (2)
			C(6)-P(2)-Ni	115.4 (3)	115.7 (3)

Dihedral Angles

atoms	293 K	135 K	atoms	293 K	135 K
Ni-N(1)-N(2) vs. Ni-P(1)-P(2)	90.4	91.2	Ni-P(1)-P(2) vs. Ni-N(2)-O(3)	82.8	88.0
Ni-N(2)-O(3) vs. Ni-N(1)-N(2)	11.5	4.8	Ni-P(1)-P(2) vs. N(1)-O(1)-O(2)	102.0	99.3
N(1)-O(1)-O(2) vs. Ni-N(1)-N(2)	32.7	32.8			

[a] Distances in angstroms and angles in degrees. Standard deviations for the distances and angles were calculated by using a variance-covariance matrix.

observed for transition-metal nitrosyl complexes[12] but is rather typical for $\{NiNO\}^{10}$ complexes.[13] These very short distances are indicative of considerable covalent bonding between nickel and the nitrosyl ligand. The nitrosyl ligand is nearly coplanar with the NiN_2 group (O(3)-N(2)-Ni/N(1)-Ni-N(2) = 11.5°, Table VI.

The Ni-N-O angle of 165.5 (8)° is also similar to those found for the closely related low-symmetry triphenylphosphine complexes $Ni(NCS)(NO)(PPh_3)_2$ (161.5 (5)°) and $Ni(N_3)(NO)(PPh_3)_2$ (152.7 (7)°), which are significantly less than the 180° observed for $\{NiNO\}^{10}$ complexes with C_{3v} or higher symmetry.[13] The Ni-N(O₂) bond distance of 1.997 (6) Å is 0.107 Å longer than the 1.890 (11) Å found[14] in

(12) Feltham, R. D.; Enemark, J. H. *Top. Stereochem.* **1981**, *12*, 155.
(13) Haller, K. J.; Enemark, J. H. *Inorg. Chem.* **1978**, *17*, 3552. Enemark, J. H. *Ibid.* **1971**, *10*, 1952. Meiners, J. H.; Rix, C. J.; Clardy, J. C.; Verkade, J. G. *Ibid.* **1975**, *14*, 705. Berglung, D.; Meek, D. W. *Ibid.* **1972**, *11*, 1493. Divaira, M.; Ghilardi, C. A.; Sacconi, L. *Ibid.* **1976**, *15*, 1555. Chong, K. S.; Retting, S. J.; Storr, A.; Trotter, J. *Can. J. Chem.* **1979**, *57*, 3090, 3107, 3113.

$Ni(NO_2)_2(DPPE)$. The NO_2 group is tipped 30° out of the plane formed by N(1)–Ni–N(2), removing any semblance of a mirror plane perpendicular to P(1)–Ni–P(2). The average Ni–P distance in **1** is also 0.063 Å longer than that found for $Ni(NO_2)_2(DPPE)$, indicative of a larger radius for the tetrahedral nickel atom of **1** compared with that of square-planar nickel complexes.[15] Within experimental error, all of the C–P–C distances and angles are the same and do not differ significantly from those reported for the five-coordinate nickel complexes reported previously.[16]

The structure found for **1** at low temperature (LT) is similar in most essential details to that found at ambient temperature, but the reduced thermal parameters, especially of the nitrosyl ligand, provide a clearer view of its molecular geometry. With the exception of Ni–P(1), the LT structure has interatomic distances that are indistinguishable from those of the room temperature (RT) structure. The Ni–P(1) distance of 2.228 (3) Å found for the LT structure differs from that found for the RT structure by 5–8σ, while the Ni–P(2) distance of 2.244 (2) Å for the LT structure is unchanged. The bond angles and dihedral angles also differ little between the LT and RT structures except for the dihedral angle of O(3)–N(2)–Ni/N(1)–Ni–N(2), which decreases from 11.5° at ambient temperature to 4.8° at 135 K (Table VI).

Discussion

Molecular Structure. The results outlined above establish that the NO_2 group is bonded to nickel through the nitrogen atom and that the nickel atom has a distorted tetrahedral geometry. The nickel nitrosyl group has a slightly bent Ni–N–O linkage well within the range found for other $\{NiNO\}^{10}$ complexes with less than 3-fold symmetry axes.[13] The bending of the Ni–N–O linkage is associated with the loss of π bonding in the direction of the plane of bending.[17] The unequal π bonding results from the disparate donor–acceptor properties of the other ligands attached to the metal, in this case PMe_3 and NO_2. The Ni–N–O groups in the other two closely related triphenylphosphine complexes, $Ni(NO)(NCS)(PPh_3)_2$ and $Ni(N_3)(NO)(PPh_3)_2$, are also similarly bent (161.5 (5) and 152.7 (7)°, respectively) in a plane that is nearly coincident with the N–Ni–X plane.[13] As was found for the other two members of this $NiX(NO)P_2$ series, there are no inter- or intramolecular contacts with the NiNO group that are close enough to cause such a large deformation. If the bending of the NiNO group is indeed due to electronic effects, then some correlation between the Ni–N distance and the NiNO angle might be expected since the loss of π bonding should also be accompanied by a lengthening of the Ni–N bond. There are now a sufficient number of structural data for the $\{NiNO\}^{10}$ complexes[12] to provide a test for this hypothesis. A plot of the Ni–N distance vs. NiNO angle for these complexes is shown in Figure 6. Although the Ni–N distance appears to increase as the NiNO angle decreases in these $\{NiNO\}^{10}$ complexes, this possible relationship should be viewed with caution since similar plots for nitrosyl complexes of other transition metals fail to evoke such a pattern.[12]

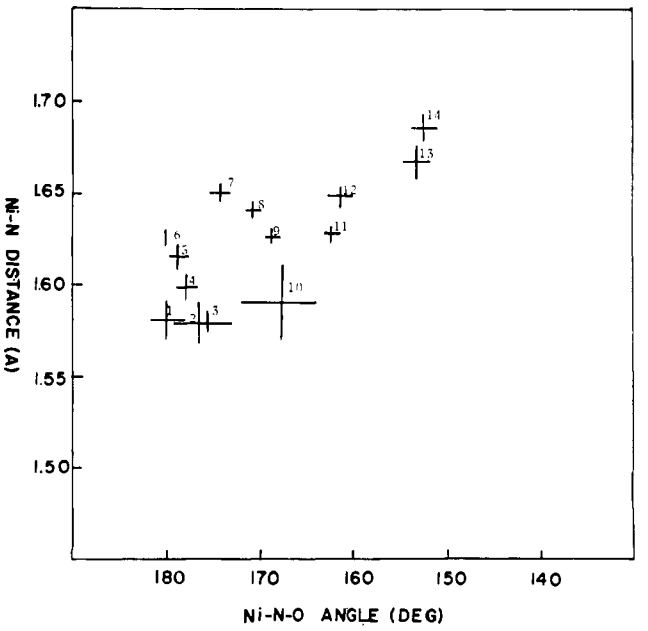

Figure 6. Ni–N (Å) vs. Ni–N–O angle (deg) for the $\{NiNO\}^{10}$ complexes. The data are taken from ref 12 and 13.

The most unusual feature of the structure of these $NiX(NO)P_2$ complexes, however, is the apparently different Ni–P distances in each. Although the two Ni–P distances found for **1** at room temperature are identical (2.243 (2) Å), they differ by 5–8σ at low temperature (2.228 (3) and 2.244 (2) Å). If **1** were the only complex to exhibit inequivalent Ni–P distances, the difference might be attributed to an experimental artifact. However, in view of the fact that each of these complexes has nonequivalent Ni–P distances, it seems likely that these differences are significant. Each of these molecules has only C_1 symmetry, so that nonequivalent Ni–P distances are permissible, but as the discussion in ref 13 points out, there are no obvious sources for the disparity in the Ni–P distances due to inter- or intramolecular contacts with other ligands; so, it appears the nonequivalence must be electronic in origin. The present complex is particularly amusing since the RT structure has equivalent Ni–P distances but has a less planar O–N–Ni–N grouping than the LT form, which has a more nearly planar O–N–Ni–N grouping but inequivalent Ni–P distances.

Taken collectively, the low symmetry adopted by $Ni(NO_2)(NO)(PMe_3)_2$ and the bending of the Ni–N–O group are in accord with the molecular orbital diagram proposed for $\{NiNO\}^{10}$ complexes in Figure 13 of ref 17. In this molecular orbital description, the HOMO consists of the filled $4a_1(d_{z^2})$ orbital of the $\{NiNO\}^{10}$ group and the LUMO is the antibonding $3e(\pi_x^*,\pi_y^*)$. The alternate form for a four-coordinate $\{NiNO\}^{10}$ complex is planar, with a strongly bent NiNO group, but this form has not been observed to date. Attainment of square-planar geometry requires $4a_1(d_{z^2})$ to be higher in energy than $3e(\pi_x^*,\pi_y^*)$, which in turn would produce a strongly bent $\{MNO\}^{10}$ group. It is clear that although the geometry of these $NiX(NO)P_2$ complexes is distorted, the coordination geometry still approximates tetrahedral. Consequently, we conclude that $4a_1(d_{z^2})$ is the HOMO but that the $3e(\pi_x^*,\pi_y^*)$ LUMO is rather close in energy, a conclusion supported by the intense absorption bands in the visible region (2.80, 2.25, and 1.75 μm^{-1}). Under these circumstances, the second-order Jahn–Teller effect proposed by Kettle[18] to describe the deviations from 180° for MCO groups in low-symmetry complexes can be operative.

(14) Kriege-Simondsen, J., submitted for publication; Drew, M. G. B.; Rogers, D. *Chem. Commun.* **1965**, 476. Drew, M. G. B.; Goodgame, D. M. L.; Hitchman, M. A.; Rogers, D. *Ibid.* **1965**, 477.

(15) The radius observed for tetrahedral Ni(II) complexes is 0.05 Å longer than that of the isomeric square-planar complex (see: Kilbourn, R. T.; Powell, H. M. *J. Chem. Soc., Dalton Trans.* **1970**, 1688). The radius found for Ni(O) complexes is even shorter than for square-planar Ni(II) (see: Kruger, C.; Tsay, Y.-H.; et al. *Cryst. Struct. Commun.* **1974**, *3*, 455. Mais, R. H. B.; Owston, P. G.; Thompson, D. T.; Wood, A. M. *J. Chem. Soc. A* **1967**, 1744; *Inorg. Chem.* **1976**, *15*, 2763).

(16) Dawson, J. K.; McLennan, T. J.; Robinson, W.; Merle, A.; Dartiguenave, M.; Dartiguenave, Y.; Gray, H. B. *J. Am. Chem. Soc.* **1974**, *96*, 4428.

(17) Enemark, J. H.; Feltham, R. D. *Coord. Chem. Rev.* **1974**, *13*, 339.

(18) Kettle, S. F. A. *Inorg. Chem.* **1965**, *4*, 1661.

Scheme I

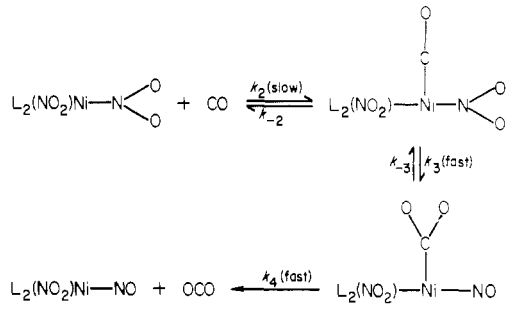

In the present case, an impending crossing of the filled $4a_1(d_{z^2})$ orbital which has a single potential minimum, with the $3e(\pi_x^*,\pi_y^*)$ orbital, which has a double potential minimum, would result in their mixing and in consequent distortion of the $\{NiNO\}^{10}$ group. Such a circumstance can lead to both bending of the NiNO group and distortion of the coordination geometry at the nickel atom in such a way as to remove the degeneracy of the $3e(\pi_x^*,\pi_y^*)$ orbital. Since in the tetrahedral geometry the $3e(\pi_x^*,\pi_y^*)$ orbital is σ antibonding with respect to the two phosphorus ligands, removal of this degeneracy could then be reflected in unequal Ni–P bond lengths. Clearly, the presence of the X ligands in these complexes has already removed the degeneracy of the 3e orbital, but each component will interact differently with $4a_1$. Further, the presence of the π-acceptor orbital on the NO_2 ligand should serve to stabilize the bonding with one or the other phosphorus ligands, provided the π^* orbital on the NO_2 group is *in the same plane* as the σ orbital of the phosphorus ligand. In both the RT and the LT structures, the NO_2 group forms a dihedral angle of 80° with the P(1)–Ni–N(1) plane, placing the π^* orbital of the NO_2 group within 10° of the plane containing the σ orbital of the P(1) ligand. Thus, the metrical details of the LT structure are in accord with the molecular orbital description.[17] A similar suggestion was forwarded for the triphenylphosphine complexes.[13] The RT structure has two Ni–P distances that are the same as the longer Ni–P(2) distance in the LT structure. This fact suggests that $Ni(NO_2)(NO)(PMe_3)_2$ may have two electronic states of similar energy with slight differences in their geometries. Some confirmation of this point of view is found in the change of orientation of the NO group as the temperature is decreased (Ni–N–O/N(1)–Ni–N(2) is 11.5° at RT and 4.8° at LT).

Reaction Mechanism. The observed rate law for the reaction of CO with both $Ni(NO_2)_2(PMe_3)_2$ and $Ni(NO_2)_2(DPPE)$ (reaction 1) is first order in CO and first order in nickel complex with values for k_2 of 6.0×10^{-1} and 2.1×10^{-1} L mol^{-1} s^{-1}, respectively. Both reactions are associative, and the nature of the phosphine ligand and the stereochemistry of the initial nickel complexes have a measurable but small influence on its rate. These observations are consistent with the mechanism proposed previously[3,4] in which the five-coordinate species $Ni(CO)(NO_2)_2L_2$ is formed in the rate-determining step (Scheme I). The enhanced rate of reaction of the trimethylphosphine complex with CO compared with that of the 1,2-bis(diphenylphosphino)ethane complex strongly supports the proposed mechanism since more basic phosphines are known to stabilize the pentacoordinate monocarbonyl complexes[1] $NiX_2(CO)L_2$.

Despite numerous attempts using a variety of spectroscopic techniques, the pentacoordinate species $Ni(CO)(NO_2)_2L_2$ has still not been observed directly. Consequently, the only information about reactions 3 and 4 (Scheme I) comes from the ^{18}O-labeling studies of Doughty et al.,[3] who showed that the carbonyl and carbon monoxide complexes were sufficiently long-lived to undergo oxygen exchange with the NO_2 ligands before CO_2 was irreversibly lost (reaction 4).

The proposed mechanism (Scheme I) indicates that under suitable conditions of solvent, temperature, and CO pressure the concentration of the pentacoordinate complex should be sufficient to be observed spectroscopically. Attempts to identify this species are continuing.

Acknowledgment. The authors are indebted to Dr. John H. Enemark for many helpful discussions, to the North Atlantic Treaty Organization, the National Science Foundation, and the Centre National de la Recherche Scientifique for financial support, and to the University of Arizona Computer Center for a generous allotment of computer time.

Registry No. **1**, 79499-32-4; **2**, 38907-60-7; CO, 630-08-0.

Supplementary Material Available: Observed and calculated structure factors for the data collected at 135 and 293 K (Tables VIII and IX), thermal parameters (Table IV), and root-mean-square amplitudes of vibration for the nonhydrogen atoms (Table VII) (19 pages). Ordering information is given on any current masthead page.